

Neural network method for determining embedding dimension of a time series



Journal:	<i>Journal of Time Series Analysis</i>
Manuscript ID:	Draft
Wiley - Manuscript type:	Original Article
Date Submitted by the Author:	
Complete List of Authors:	Maus, Adam; University of Wisconsin - Madison, Physics Sprott, Julien; University of Wisconsin - Madison, Physics
Keywords:	embedding dimension, neural network, lag space, chaos
Abstract:	<p>A method is described for determining the optimal time-delay embedding dimension for a scalar time series by training an artificial neural network on the data and then determining the sensitivity of the output of the network to each time lag averaged over the data set. As a byproduct, the method identifies any intermediate time lags that do not influence the dynamics, thus permitting a possible further reduction in the required embedding dimension. The method is tested on four sample data sets and compares favorably with more conventional methods including false nearest neighbors and the 'plateau dimension' determined by saturation of the calculated correlation dimension. The proposed method is especially advantageous when the data set is small or contaminated by noise. The trained network could be used for noise reduction, forecasting, and estimating the dynamical and topological properties of the system that produced the data, such as the Lyapunov exponent, entropy, and attractor dimension.</p>

Neural network method for determining embedding dimension of a time series

A. Maus and J. C. Sprott

Physics Department, University of Wisconsin, 1150 University Avenue, Madison, Wisconsin, 53706, USA

A method is described for determining the optimal time-delay embedding dimension for a scalar time series by training an artificial neural network on the data and then determining the sensitivity of the output of the network to each time lag averaged over the data set. As a byproduct, the method identifies any intermediate time lags that do not influence the dynamics, thus permitting a possible further reduction in the required embedding dimension. The method is tested on four sample data sets and compares favorably with more conventional methods including false nearest neighbors and the ‘plateau dimension’ determined by saturation of the calculated correlation dimension. The proposed method is especially advantageous when the data set is small or contaminated by noise. The trained network could be used for noise reduction, forecasting, and estimating the dynamical and topological properties of the system that produced the data, such as the Lyapunov exponent, entropy, and attractor dimension.

I. INTRODUCTION

When presented with an experimental time series from which one wants to make a forecast or determine properties of the underlying dynamical system, the starting point is usually to embed the data in a time-delayed space of suitable dimension (Packard *et al.*, 1980). If this embedding dimension is chosen too small, distant points on the attractor will coincide or overlap in the embedding space like the 2-dimensional shadow of a 3-dimensional object. However, if it is chosen too large, the space may be poorly sampled, noise will be more problematic, and more computation is required. Consequently, it is important to choose an optimal embedding dimension.

A sufficient condition for the embedding dimension was provided by Takens (1981) who showed that complete unfolding is guaranteed if the time-delayed embedding space has a dimension d greater than the dimension of the original state space D by an amount $d > 2D$. Sauer *et al.* (1991) later showed that under most conditions, the embedding dimension need only be greater than twice the fractal dimension of the attractor. However, it is important to recognize

1
2
3 that for many purposes, such as calculation of the correlation dimension (Grassberger *et al.*,
4 1983), overlaps are of little consequence if their measure is sufficiently small, and in such cases,
5
6 the necessary embedding dimension may be as small as the next integer larger than the
7
8 dimension of the attractor.
9
10

11
12 A closely related issue is determining the extent to which each time lag influences the
13 future. It is easy to imagine situations in which intermediate time lags are of no consequence, for
14
15 example in biological systems where seasonal, gestation, or maturation delays are present
16
17 (Allman *et al.*, 2004). In such cases the relevant ‘lag space’ may in fact be smaller than the
18
19 embedding dimension estimated by conventional methods since the attractor may be negligibly
20
21 thin in some of the intermediate dimensions. Therefore, the dimension of the lag space indicates
22
23 the number of variables needed to model the dynamics. Methods developed for linear systems
24
25 such as the autocorrelation function and autoregressive moving average (ARMA) models (Box *et*
26
27 *al.*, 1994) naturally provide such information, but our interest here is in more general methods
28
29 that work for nonlinear systems, and in particular, ones that exhibit chaos for which the linear
30
31 methods would miserably fail. A byproduct of using the neural network method to find the
32
33 optimal embedding dimension is determination of the lag space.
34
35
36
37
38
39
40

41 One of the earliest methods for determining an optimal embedding dimension is to
42
43 calculate the correlation dimension in increasing embeddings and to declare that the proper
44
45 embedding has been found when the calculated correlation dimension saturates. This ‘plateau
46
47 dimension’ by its nature is optimal for determining the true correlation dimension of the
48
49 attractor, but it may not adequately remove overlaps for other purposes. Furthermore, a good
50
51 plateau is often lacking with real data, especially when the data set is small and/or contaminated
52
53 with noise.
54
55
56
57
58
59
60

1
2
3 A more recent and commonly used method involves calculation of false nearest
4 neighbors (Abarbanel, 1996; Cellucci *et al.*, 2003) in successively higher embedding dimensions
5 and its many variants. Neighbors are considered false if their separation increases by more than a
6 factor of R_T when the embedding dimension is increased from j to $j+1$, where R_T is typically
7 taken as 15. In addition, a neighbor is considered false if its separation increases by more than a
8 factor of A_T times the standard deviation of the data, where A_T is typically taken as 2.0 (Kennel,
9 1992). In practice, as j is increased, the fraction of neighbors that are false drops to near zero, and
10 the dimension where this occurs is the optimal embedding dimension.
11
12
13
14
15
16
17
18
19
20
21

22 II. NEURAL NETWORK METHOD

23
24 In this paper, we propose an alternate method using a single-layer, feed-forward artificial
25 neural network trained on time-delayed data and optimized for next-step prediction based on d
26 time lags, with d chosen large enough to capture the relevant dynamics but much smaller than
27 the number of data points in the time-series c . Analysis of the trained network then allows
28 determination of the optimal embedding, lag space, and the sensitivity of the output of the
29 network to each time lag.
30
31
32
33
34
35
36
37
38

39 Artificial neural networks have shown great promise in modeling time-series (Troncia *et*
40 *al.*, 2003; Principe *et al.*, 1994), nonlinear prediction (Zhang *et al.*, 1998), and the analysis of
41 underlying features of data (Principe *et al.*, 1992). Hornik, *et al.* (1990) proved that neural
42 networks are ‘universal approximators’ because they can represent any smooth function to
43 arbitrary precision given sufficiently many neurons. Thus we believe the method is general and
44 applicable to most real-world systems.
45
46
47
48
49
50
51
52

53 The single-layer, feed-forward network shown schematically in figure 1 uses a layer of n
54 hidden neurons to perform next step prediction \hat{x}_k on a scalar time-series x_k according to
55
56
57
58
59
60

$$\hat{x}_k = \sum_{i=1}^n b_i \tanh \left(a_{i0} + \sum_{j=1}^d a_{ij} x_{k-j} \right), \quad (1)$$

where a_{ij} is an $n \times d$ matrix of coefficients, and b_i is a vector of length n . The a_{ij} matrix represents the connection strengths to the input of the network, and the b_i vector is used to control the contribution of each neuron to the output of the network. The vector a_{i0} is an offset that facilitates training on data whose mean is not zero.

The weights in a and b are updated using a method similar to simulated annealing in which a Gaussian neighborhood of the current best solution is randomly searched, with the size of the neighborhood slowly shrinking as training progresses. In practice, the Gaussian is taken to have an initial standard deviation of 2^{-j} centered on zero to give preference to the most recent time lags (small j values) in the search space. The connection strengths are chosen to minimize the average one-step mean-square prediction error:

$$e = \frac{\sum_{k=d+1}^c (\hat{x}_k - x_k)^2}{c - d} \quad (2)$$

Once the network is trained, the sensitivity of the output to each time lag is determined by calculating the partial derivatives of the output with respect to each time lag x_{k-j} averaged over all the points in the time-series:

$$\hat{S}(j) = \frac{1}{c - j} \sum_{k=j+1}^c \left| \frac{\partial \hat{x}_k}{\partial x_{k-j}} \right| \quad (3)$$

For the network in equation 1 the partial derivatives are given by

$$\frac{\partial \hat{x}_k}{\partial x_{k-j}} = \sum_{i=1}^n a_{ij} b_i \operatorname{sech}^2 \left(a_{i0} + \sum_{m=1}^d a_{im} x_{k-m} \right) \quad (4)$$

1
2
3
4 The optimal embedding dimension is assumed to be the largest value of j for which $\hat{S}(j)$ has a
5
6 significant value much like the method of false nearest neighbors. The individual values of $\hat{S}(j)$
7
8 quantify the importance of each time lag, much like the terms in the autocorrelation function or
9
10 the coefficients of an ARMA model for a linear system.
11
12

13 14 III. NUMERICAL RESULTS

15
16 The method was tested on four time-delayed chaotic maps of increasing dimension and
17
18 complexity. One advantage of using data generated in this way is that the expected sensitivities
19
20 to each time lag $S(j)$ can be readily determined either by inspection of the equation that
21
22 generated the data in cases where the dependence is linear or by a simple numerical averaging of
23
24 the nonlinear terms over the points on the attractor using equation 3. The attractor produced by
25
26 many iterations of the trained network is visually indistinguishable from the one that produced
27
28 the time series. The next-step, in-sample prediction error calculated from equation for all these
29
30 noise-free cases is on the order of $e \sim 10^{-5}$. For each map, ten different instances of the time
31
32 series were taken, and the neural networks' sensitivities to each time lag were calculated. This
33
34 resulted in an average normalized root mean square error in the calculated sensitivities, equation
35
36 9, less than 0.0354 with a variance less than 0.0210 for each map, with the figures representing
37
38 the average of the ten trials. In addition, the finite-size Lyapunov exponent (Aurell *et al.*, 1997;
39
40 Ziehmman *et al.*, 2000) for the trained network is in agreement with the expected value within
41
42 5% over the range of scale sizes from 10^{-12} to 10^{-1} .
43
44
45
46
47
48

49 The network parameters n and d , and the number of data points c used to model the cases
50
51 to be shown were chosen for their ability to produce an accurate model of the system. There is a
52
53 tradeoff between accuracy and the time required to train the network. If n , d , or c are too small,
54
55 the network will train poorly and give inaccurate sensitivities. For n , d , or c too large,
56
57
58
59
60

1
2
3 degradation in the model will result from insufficient training or from over-fitting. Except as
4
5 noted, we use the values of $n = 4$, $d = 5$, and $c = 512$, which appear adequate for the cases
6
7 studied, but are not necessarily optimal even for these cases. In particular, we note that the
8
9 number of neurons required to get good agreement in the sensitivities is smaller than the number
10
11 required for the smallest training error e , presumably because the goal is not to get the best fit to
12
13 the data but only to determine the sensitivity to each time lag. In practice, one should try
14
15 different values of the parameters for each time series, but we find the method is tolerant of a
16
17 wide range of choices.
18
19
20

21
22 The simplest case considered here is the Hénon map (Hénon, 1976), given in time-
23
24 delayed form by

$$25 \quad x_k = 1 - 1.4x_{k-1}^2 + 0.3x_{k-2}, \quad (5)$$

26
27 with a strange attractor as shown in figure 2(a). From equation 5 it is evident that this map has an
28
29 optimal embedding and lag-space dimension of 2 since two time lags uniquely determine each
30
31 value of x_k . The expected sensitivities to the two lags are $S(1) = 1.8959$ and $S(2) = 0.3$,
32
33 respectively.
34
35
36
37

38
39 Figure 3(a) shows that the values of $\hat{S}(j)$ predicted by the neural network are in near
40
41 perfect agreement with the expected values. In particular, $\hat{S}(j) < 2 \times 10^{-3}$ for $j > 2$. Error bars
42
43 representing the standard deviation of the ten cases that were evaluated are not shown because
44
45 they are negligibly small, typically about 1%. Figure 3(b) shows values of $F(j)$, defined as the
46
47 fraction of neighbors that were false in dimension $j-1$, plotted in this unconventional way so that
48
49 the fraction reaches zero when the optimal embedding is obtained to simplify the comparison
50
51 with $\hat{S}(j)$. Figure 3(c) shows the difference in calculated correlation dimension $\Delta D_2 = D_2(j) -$
52
53 $D_2(j-1)$, which is expected to fall to zero once j exceeds the optimal embedding dimension,
54
55
56
57
58
59
60

1
2
3 indicating that a plateau in the calculated D_2 has been reached. All three methods accurately
4
5 predict an optimal embedding of 2.
6
7

8 Since the Hénon map is a relatively trivial example, the method was tested on several
9
10 additional cases of increasing dimension and complexity. The first of these is the three-
11
12 dimensional chaotic map from the preface from Sprott (2003) whose form
13
14

$$15 \quad x_k = x_{k-1}^2 - 0.2x_{k-1} - 0.9x_{k-2} + 0.6x_{k-3}, \quad (6)$$

16
17 gives the strange attractor shown in figure 2(b) with an optimal embedding dimension of 3. The
18
19 expected sensitivities are $S(1) = 1.1502$, $S(2) = 0.9$, and $S(3) = 0.6$. Figure 4 compares the three
20
21 methods, and they show reasonable agreement, except that the plateau for the correlation
22
23 dimension appears to be closer to 2 than to 3 as expected since the attractor has a dimension less
24
25 than 2, and hence the overlaps are a set of measure zero.
26
27
28

29
30 A four-dimensional example in which the lag space is less than the optimal embedding
31
32 dimension is the delayed Hénon map (Sprott, 2006),
33
34

$$35 \quad x_k = 1 - 1.6x_{k-1}^2 + 0.1x_{k-4}, \quad (7)$$

36
37 with an attractor shown in figure 2(c). The dynamics of the map only depend on the first and
38
39 fourth time lags. The expected sensitivities are $S(1) = 1.9018$ and $S(4) = 0.1$.
40
41

42 Figure 5 shows that only the neural network method identifies the gap in the time lags
43
44 where the sensitivities that should be zero, $\hat{S}(2)$ and $\hat{S}(3)$, are an order of magnitude smaller
45
46 than $\hat{S}(4)$. Unlike the saturation of the correlation dimension, false nearest neighbors accurately
47
48 identifies 4 as the optimal embedding dimension. Another case (not shown) is a delayed Hénon
49
50 map with an extremely long delay of 80, having expected sensitivities $S(1) = 1.9018$ and $S(80) =$
51
52
53
54
55
56
57
58
59
60
0.1. The sensitivities predicted by the trained network are $\hat{S}(1) = 1.6985$ and $\hat{S}(80) = 0.1035$,

with all intermediate lags on the order of 10^{-3} or less. For this case, the neural network had 4 neurons, 80 dimensions, and a training error of 2.6212×10^{-3} , although more accurate sensitivities are likely with further training.

The final example is a four-dimensional variation of the Hénon map studied by Goutte (1997) and given by

$$x_k = 1 - 1.4x_{k-2}^2 + 0.3x_{k-4}, \quad (8)$$

which, like the delayed Hénon map, has gaps in its lag space. Its strange attractor as shown in figure 3(d) consists of two coexisting and non-interacting Hénon maps, one for odd k and the other for even k . The expected sensitivities are $S(2) = 1.8959$ and $S(4) = 0.3$, the same as for the simple Hénon map but with different lags.

Figure 6 shows that the neural network method works very well, while the other two methods predict an incorrect embedding of 3. Only the neural network method correctly identifies the gaps in the time lags. It is remarkable that with only four neurons, the neural network is able to accurately model two co-mingled two-dimensional nonlinear maps.

IV. DATA REQUIREMENTS AND NOISE

In the real world, data records are often short and contaminated with noise. The performance of the various methods was tested using time series for the simple Hénon map of different lengths and with added noise. The performance was compared by calculating the normalized root mean square error for each method. For example, the error for the neural network method is given by

$$E = \sqrt{\frac{\sum_{j=1}^d (\hat{S}(j) - S(j))^2}{\sum_{j=1}^d S^2(j)}}, \quad (9)$$

1
2
3 and similarly for the other two methods. For false nearest neighbors, the expected values were
4
5 determined from a calculation using 6000 noise-free data points from the simple Hénon map. For
6
7 the correlation dimension, the expected values were determined from a calculation using 10 000
8
9 data points from the simple Hénon map.
10
11

12
13 Figure 7 shows the performance of the three methods for varying amounts of data. The
14
15 neural network method works almost perfectly even with as few as 32 data points, whereas the
16
17 other methods seriously degrade when the number is less than several hundred.
18
19

20
21 In all the previous examples, the neural network had fixed values of n and d , chosen to be
22
23 adequate for the cases studied. With experimental data, one would not typically know in advance
24
25 how to choose d in particular. In such a case, one would train the network with increasing values
26
27 of d , looking for a knee in a plot of the error e versus d , signifying that an adequate embedding
28
29 had been achieved, much as one does for false nearest neighbors and for the correlation
30
31 dimension. Figure 8 shows such a plot for a variant of the delayed Hénon map in equation 7, but
32
33 with a delay of 5,
34
35

$$36 \quad x_k = 1 - 1.6x_{k-1}^2 + 0.1x_{k-5} \quad (10)$$

37
38 This modification results in expected sensitivities $S(1) = 1.9018$ and $S(5) = 0.1$. Figure 8 shows
39
40 that as d is increased with $n = 4$ and $c = 512$, the root mean square error e falls by a factor of 100
41
42 at $d = 5$ and remains at that level, signifying that the optimal embedding was reached. The
43
44 normalized root mean square error E in the sensitivities $S(j)$ increases slightly and then falls by a
45
46 factor of 2 at $d = 5$. The knee would have been even more pronounced for a map with a larger
47
48 value of $S(5)$, which in this case is only about 5% of $S(1)$.
49
50
51
52

53
54 To compare the methods in the presence of noise, Gaussian white noise of varying
55
56 amounts was added to a time-series with $c = 512$ from the simple Hénon map using equation 9
57
58
59
60

1
2
3 to compare the three methods, where the expected values were taken from a noiseless case with
4
5 512 data points from the simple Hénon map. The results in figure 9 show that the neural network
6
7 method is considerably more robust to noise than are the other methods, but as the signal-to-
8
9 noise ratio approaches unity, it too fails.
10
11

12
13 Since it is well known that colored noise can masquerade for low dimensional chaos
14
15 (Osborne *et al.*, 1989), the same experiment was performed with integrated white noise (also
16
17 known as Brownian or $1/f^2$ noise) with the results shown in figure 10. The superiority of the
18
19 neural network method over the other methods is even more evident than for the case with white
20
21 noise, probably because the noise is concentrated at low frequencies and is relatively small in the
22
23 band of frequencies occupied by the signal. Presumably, this result would also hold for other
24
25 forms of colored noise.
26
27

28
29 The typical error bars in figures 9 and 10 at a signal-to-noise ratio of 7 dB indicate the
30
31 standard deviation from the mean of ten different instances of the time series (different chaos and
32
33 different noise) for each of the indicated cases. It is not surprising that the neural network
34
35 completely removes the noise and gives a low-dimensional attractor since it is entirely
36
37 deterministic, but at the expense of some distortion of the signal. Any method that fits a
38
39 deterministic model to data by its nature will be noise-free, and thus noise reduction is a
40
41 byproduct of the method proposed here.
42
43
44

45
46 With real-world data, it is not usually clear what is signal and what is noise, and thus one
47
48 can never be confident how much of the difference between the model and the data is really
49
50 noise. For that purpose, a number of additional metrics have been proposed including the (ϵ, τ) -
51
52 entropy (Gaspard *et al.*, 1993; Cencini *et al.*, 2000), which generalizes the Kolmogorov-Sinai
53
54 entropy, the finite-size Lyapunov exponent (Aurell *et al.*, 1997; Ziehmman *et al.*, 2000), which
55
56
57
58
59
60

1
2
3 reduces errors due to low-level noise, and the scale-dependent Lyapunov exponent (Gao *et al.*,
4
5 2006), which extends the finite-size Lyapunov exponent to a range of sizes and is especially
6
7 useful for short time series. These metrics may sometimes be useful for avoiding errors in the
8
9 embedding caused by noise and to optimize the noise reduction, but they are not required for the
10
11 systems studied in this paper since we have the luxury of knowing the correct embedding
12
13 directly from the form of the maps that were used to test the method.
14
15

16 17 18 **V. CONCLUSIONS**

19
20 A proposed neural network method for determining the optimal embedding dimension
21
22 and lag space was tested for time series generated from various chaotic time-delayed maps and
23
24 was found to work almost perfectly, even with a very small number of neurons. This method
25
26 performs much better than false nearest neighbors and the plateau in the correlation dimension,
27
28 neither of which are capable of determining gaps in the embedding dimension. Furthermore, the
29
30 neural network method gives quantitative information about the relative importance of each time
31
32 lag in forecasting, which the other methods do not. When the time series is short and/or
33
34 contaminated by noise, the neural network method degrades more gracefully than the other
35
36 methods.
37
38

39
40 We finally remark that the method does not require that the model be a neural network or
41
42 that it use a hyperbolic function activation function. If one has the luxury of having a physically
43
44 based model for the system under study, it is almost always a good idea to use that model rather
45
46 than a general one such as a neural network, but it must be a model of sufficiently high
47
48 dimension with a corresponding large number of parameters.
49
50

51
52 It remains to be seen how well the method works for more complicated observer
53
54 functions or those obtained from sampling a continuous-time system where more complicated
55
56
57
58
59
60

1
2
3 network architectures may be required. Even more interesting is to apply the method to time
4 series records from experimental or observational data. These studies are beyond the scope of
5
6 this paper and will be the subject of future publications.
7
8
9

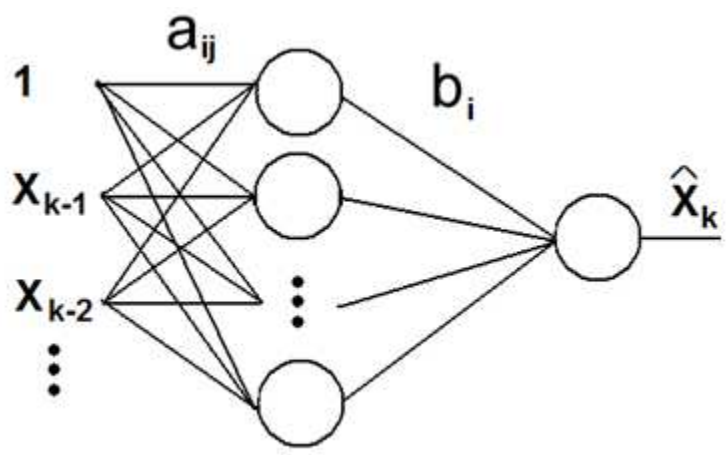
10 REFERENCES

- 11
12 Abarbanel, H. Brown, R., Sidorowich, J. J., and Tsimring, L. S. (1993) The analysis of observed
13 chaotic data in physical systems. *Reviews of Modern Physics* **65**, 1331–1392.
14
15
16
17 Allman, E. S. and Rhodes, J. A. (2004) *Mathematical Models in Biology: An Introduction*.
18 Cambridge: Cambridge University Press.
19
20
21 Aurell, E., Boffetta, G., Crisanti, A., Paladin, G., and Vulpiani, A. (1997) Predictability in the
22 large: an extension of the concept of Lyapunov exponent. *Journal of Physics A:*
23 *Mathematical and General* **30**, 1–26.
24
25
26
27
28 Box, G. E. P., Jenkins, G. M., and Reinsel, G. C. (1994) *Time-series Analysis: Forecasting and*
29 *Control, 3rd edition*. Hoboken: John Wiley & Sons, Inc.
30
31
32
33 Cellucci, C. J., Albano, A. M., and Rapp, P. E. (2003) Comparative study of embedding
34 methods. *Physical Review E* **67**, 066210.
35
36
37
38 Cencini, M., Falcioni, M., Olbrich, E., Kantz, H., and Vulpiani, A. (2000) Chaos or noise:
39 Difficulties of a distinction. *Physical Review E* **62**, 427–437.
40
41
42
43 Gao, J. B., Hu, J., Tung, W. W., and Cao, Y.H. (2006) Distinguishing chaos from noise by scale-
44 dependent Lyapunov exponent. *Physical Review E* **74**, 066204.
45
46
47
48 Gaspard, P. and Wang, X.-J. (1993) Noise, chaos, and (ε, τ) -entropy per unit time. *Physics*
49 *Reports* **235**, 291–343.
50
51
52
53 Grassberger, P. and Procaccia, I. (1983) Measuring the strangeness of strange attractors. *Physica*
54 *D* **9**, 189–208.
55
56
57
58
59
60

- 1
2
3 Goutte, C. (1997) Lag space estimation in time series modelling. In *IEEE International*
4
5 *Conference on Acoustics, Speech, and Signal Processing 4* (ed B. Werner). Munich, pp.
6
7 3313-3316.
8
9
10 Hénon, M. (1976) A two-dimensional mapping with a strange attractor. *Communications in*
11
12 *Mathematical Physics* **50**, 69–77.
13
14
15 Hornik, K., Stinchcombe, M., and White, H. (1990) Multilayer feedforward networks are
16
17 universal approximators. *Neural Networks* **3**, 535–549.
18
19
20 Kennel, M., Brown, R., and Abarbanel, H. (1992) Determining embedding dimension for phase-
21
22 space reconstruction using a geometrical construction. *Physical Review A* **45**, 3403–3411.
23
24
25 Osborne, A. R. and Provenzale, A. (1989) Finite correlation dimension for stochastic systems
26
27 with power-law spectra. *Physica D* **35**, 357–381.
28
29
30 Packard, N. H., Crutchfield, J. P., Farmer, J. D., and Shaw, R. S. (1980) Geometry from a time
31
32 series. *Physical Review Letters* **45**, 712–716.
33
34
35 Principe, J. and Kuo, J. (1995) Dynamic modelling of chaotic time series with neural networks.
36
37 In *Advances in Neural Information Processing Systems 7* (eds G. Tesauro, D. Touretzky, and
38
39 T. Leen). Denver: MIT Press, pp. 311.
40
41
42 Principe, J., Rathie, A., and Kuo, J. (1992) Prediction of chaotic time series with neural networks
43
44 and the issue of dynamic modeling. *International Journal of Bifurcation and Chaos* **2**, 989–
45
46 996.
47
48
49 Sauer, T., Yorke, J., and Casdagli, M. (1991) Embedology. *Journal of Statistical Physics* **65**,
50
51 570–616.
52
53
54 Sprott, J. C. (2003) *Chaos and Time-Series Analysis*. New York: Oxford University Press.
55
56
57
58
59
60

- 1
2
3
4
5
6
7
8
9
10
11
12
13
14
15
16
17
18
19
20
21
22
23
24
25
26
27
28
29
30
31
32
33
34
35
36
37
38
39
40
41
42
43
44
45
46
47
48
49
50
51
52
53
54
55
56
57
58
59
60
- Sprott, J. C. (2006) High-dimensional dynamics in the delayed Hénon map. *Electronic Journal of Theoretical Physics* **3**, 19–35.
- Takens, F. (1981) Detecting strange attractors in turbulence. In *Dynamical Systems and Turbulence Volume 898* (eds D. A. Rand and L. S. Young). Heidelberg: Springer Berlin, pp. 366-381.
- Troncia, S., Gionab, M., and Barata, R. (2003) Reconstruction of chaotic time series by neural models: a case study. *Neurocomputing* **55**, 3–4.
- Zhang, G., Patuwo, B., and Hu, M. (1998) Forecasting with artificial neural networks: The state of the art. *International Journal of Forecasting* **14**, 35–62.
- Ziehmann, C., Smith, L. A., and Kurths, J. (2000) Localized Lyapunov exponents and the prediction of predictability. *Physics Letters A* **271**, 237–251.

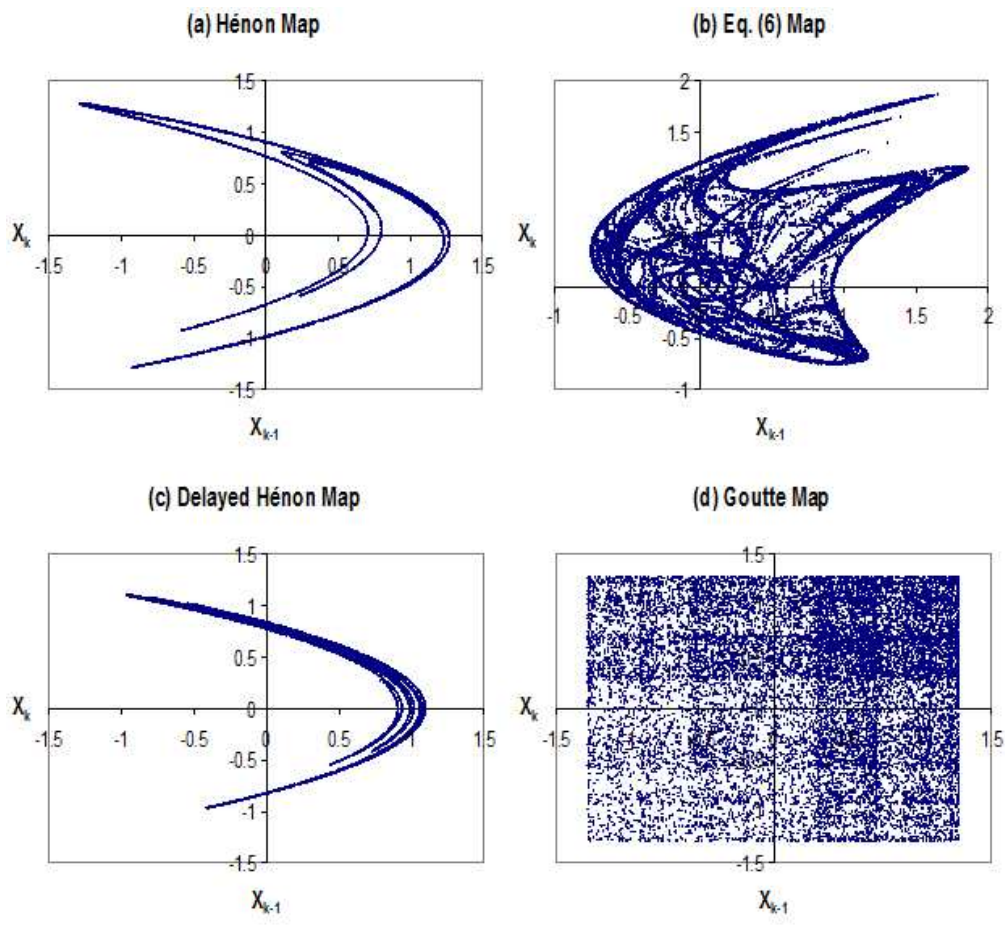
1
2
3
4
5
6
7
8
9
10
11
12
13
14
15
16
17
18
19
20
21
22
23
24
25
26
27
28
29
30
31
32
33
34
35
36
37
38
39
40
41
42
43
44
45
46
47
48
49
50
51
52
53
54
55
56
57
58
59
60



Single layer, feed-forward neural network
133x83mm (72 x 72 DPI)

Review Only

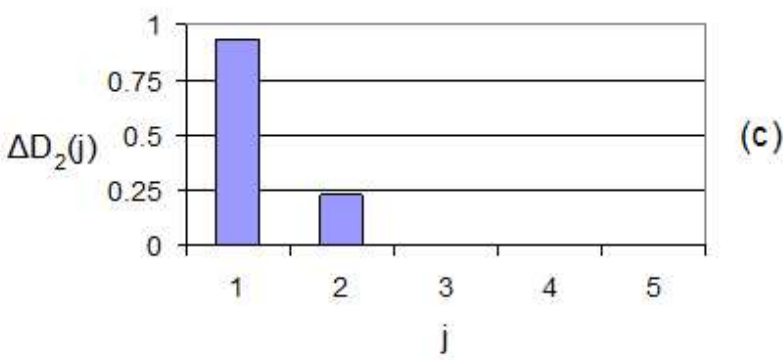
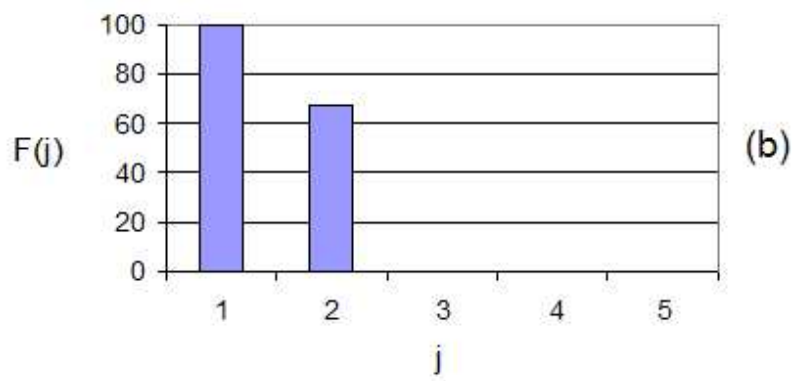
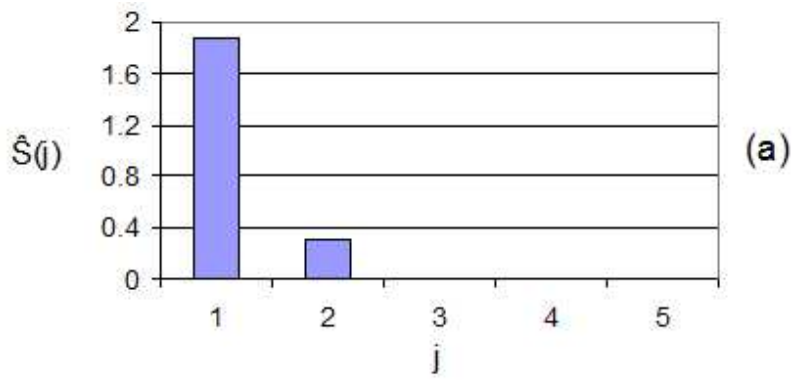
1
2
3
4
5
6
7
8
9
10
11
12
13
14
15
16
17
18
19
20
21
22
23
24
25
26
27
28
29
30
31
32
33
34
35
36
37
38
39
40
41
42
43
44
45
46
47
48
49
50
51
52
53
54
55
56
57
58
59
60



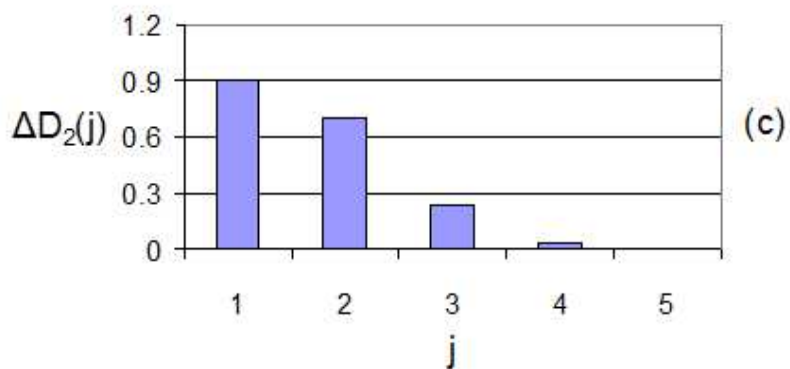
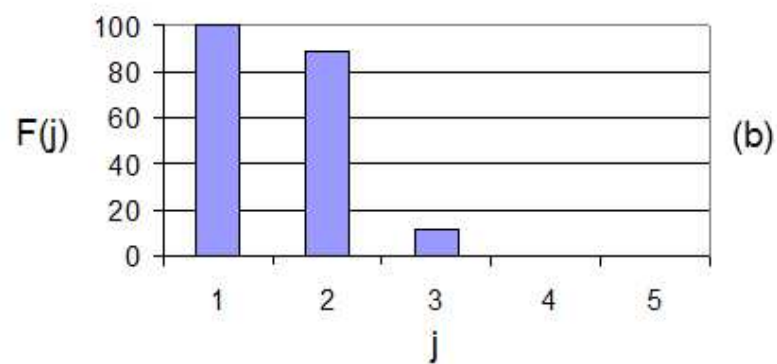
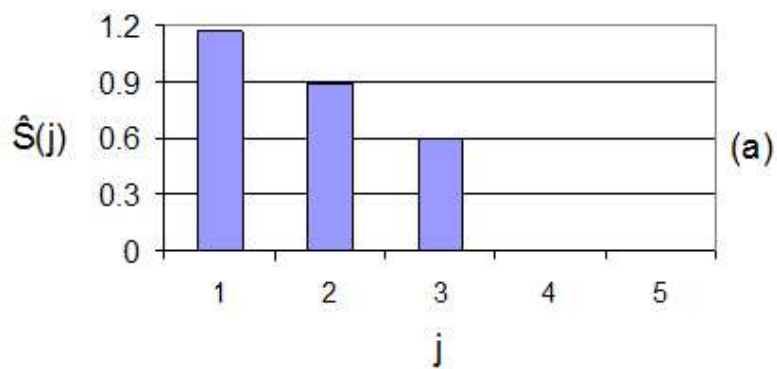
Strange attractors of maps studied
218x201mm (72 x 72 DPI)



1
2
3
4
5
6
7
8
9
10
11
12
13
14
15
16
17
18
19
20
21
22
23
24
25
26
27
28
29
30
31
32
33
34
35
36
37
38
39
40
41
42
43
44
45
46
47
48
49
50
51
52
53
54
55
56
57
58
59
60

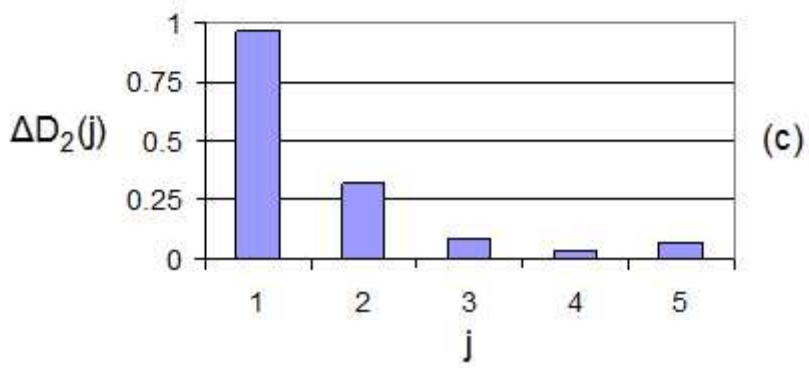
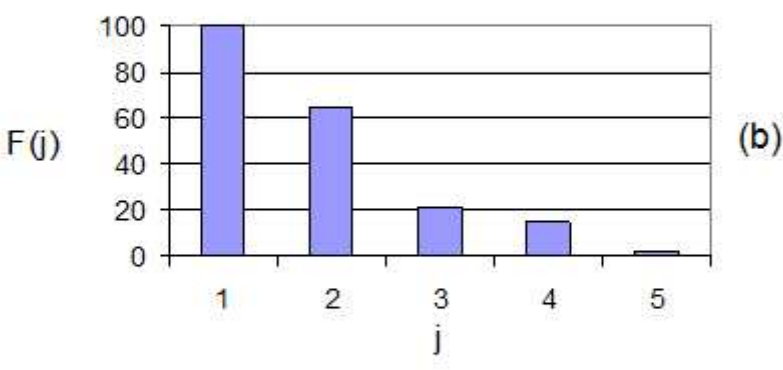
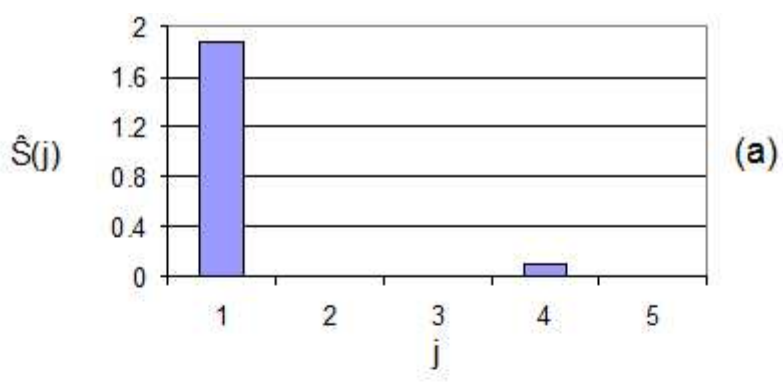


Embedding calculations for the simple Hénon map using (a) Neural network sensitivities (b) False nearest neighbors (c) Correlation dimension
149x216mm (72 x 72 DPI)

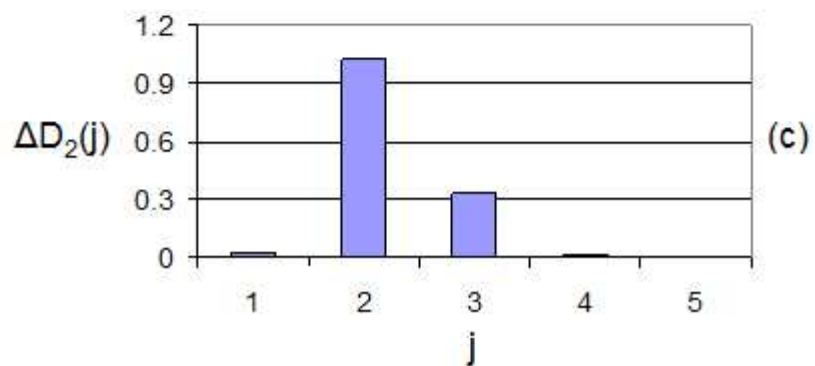
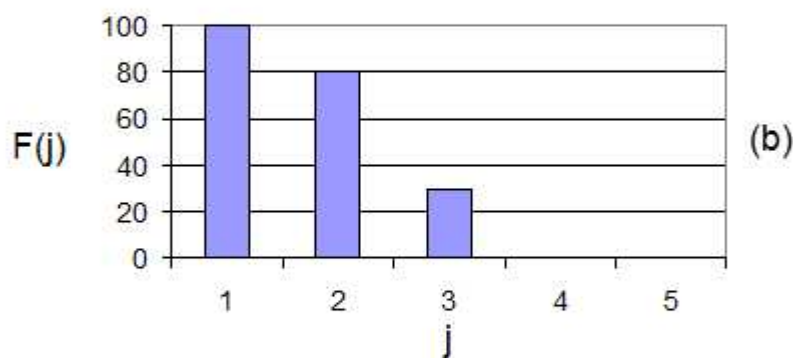
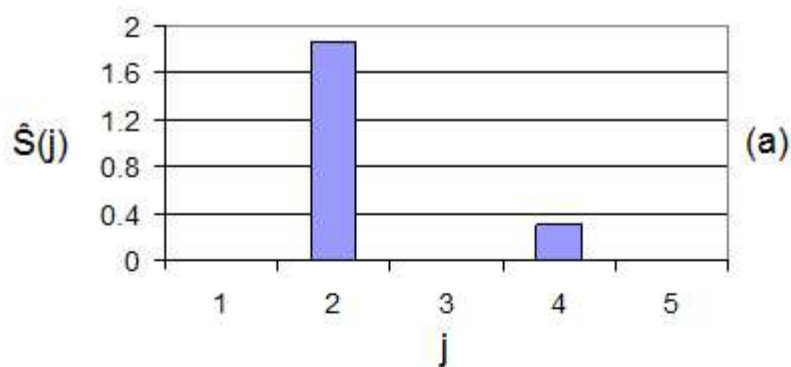


48 Embedding calculations for Eq. (6) using (a) Neural network sensitivities (b) False nearest neighbors
49 (c) Correlation dimension
50 151x223mm (72 x 72 DPI)

1
2
3
4
5
6
7
8
9
10
11
12
13
14
15
16
17
18
19
20
21
22
23
24
25
26
27
28
29
30
31
32
33
34
35
36
37
38
39
40
41
42
43
44
45
46
47
48
49
50
51
52
53
54
55
56
57
58
59
60



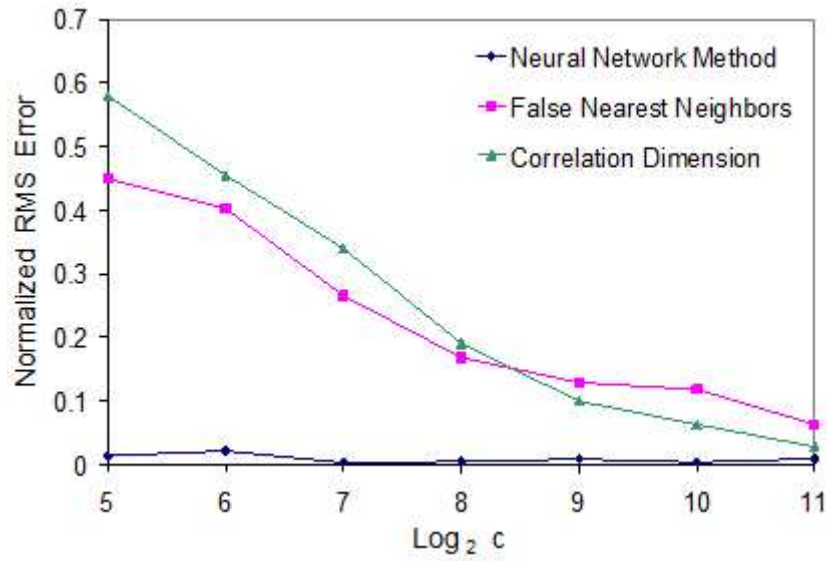
Embedding calculations for the delayed Hénon map using (a) Neural network sensitivities (b) False nearest neighbors (c) Correlation dimension
149x208mm (72 x 72 DPI)



47
48
49
50
51
52
53
54
55
56
57
58
59
60

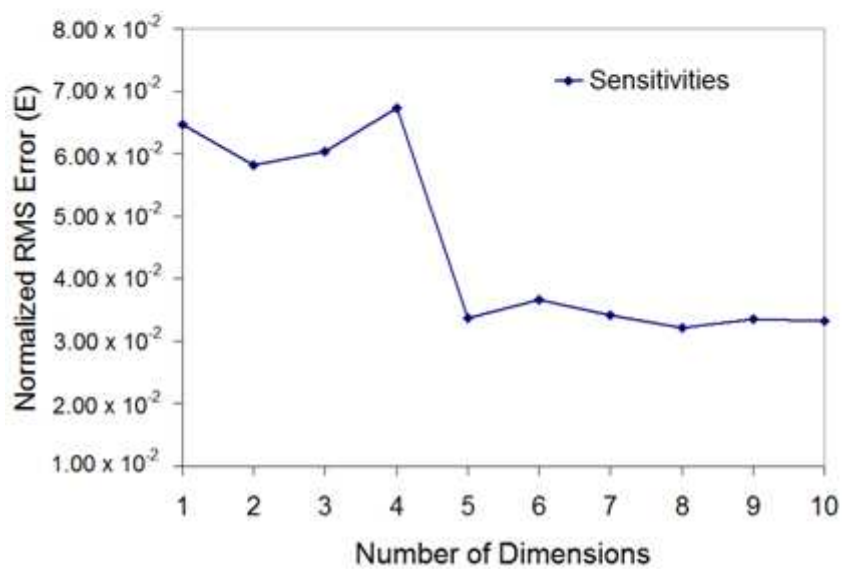
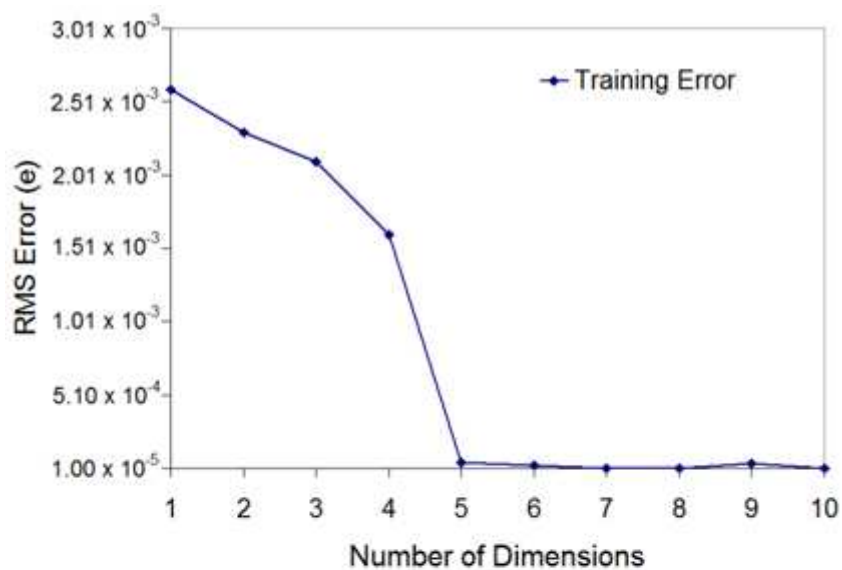
Embedding calculations for the Goutte map using (a) Neural network sensitivities (b) False nearest neighbors (c) Correlation dimension
147x210mm (72 x 72 DPI)

1
2
3
4
5
6
7
8
9
10
11
12
13
14
15
16
17
18
19
20
21
22
23
24
25
26
27
28
29
30
31
32
33
34
35
36
37
38
39
40
41
42
43
44
45
46
47
48
49
50
51
52
53
54
55
56
57
58
59
60



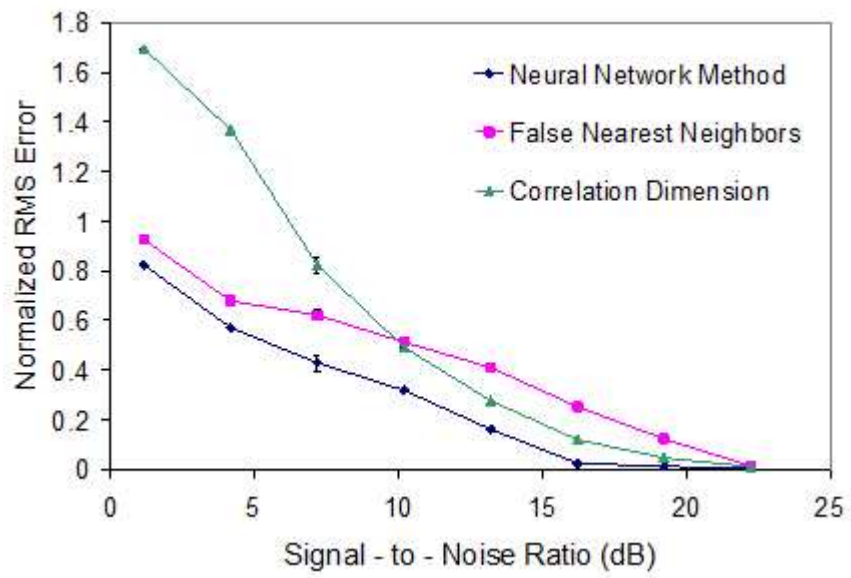
Comparison of three methods for calculating embedding dimension versus length of the time series c for the Hénon map
148x102mm (72 x 72 DPI)

View Only



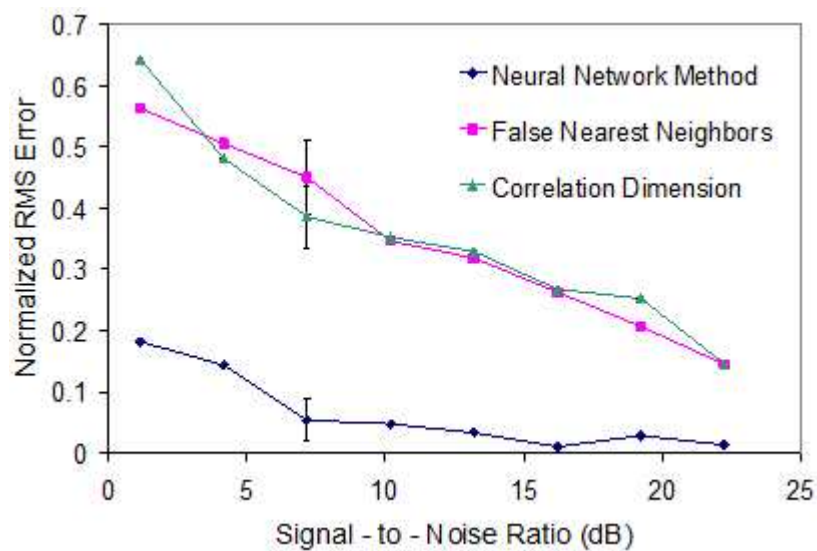
Change in neural network training error and error in sensitivities with varying dimensions for the delayed Hénon map
148x206mm (72 x 72 DPI)

1
2
3
4
5
6
7
8
9
10
11
12
13
14
15
16
17
18
19
20
21
22
23
24
25
26
27
28
29
30
31
32
33
34
35
36
37
38
39
40
41
42
43
44
45
46
47
48
49
50
51
52
53
54
55
56
57
58
59
60



Comparison of three methods for calculating embedding dimension in the presence of varying degrees of white noise for the Hénon map
151x105mm (72 x 72 DPI)

Pre-view Only



Comparison of three methods for calculating embedding dimension in the presence of varying degrees of Brownian noise for the Hénon map
143x99mm (72 x 72 DPI)

View Only